Energy & Environmental Science

COMMUNICATION

View Article Online
View Journal | View Issue

Cite this: *Energy Environ. Sci.*, 2016, **9**, 2545

Received 22nd June 2016,
Accepted 6th July 2016

DOI: 10.1039/c6ee01800a

www.rsc.org/ees

Promising prospects for 2D d^2–d^4 M_3C_2 transition metal carbides (MXenes) in N_2 capture and conversion into ammonia†

Luis Miguel Azofra,[a] Neng Li,[b] Douglas R. MacFarlane[a] and Chenghua Sun*[a]

Density functional theory investigations of M_3C_2 transition metal carbides from the d^2, d^3, and d^4 series suggest promising N_2 capture behaviour, displaying spontaneous chemisorption energies that are larger than those for the capture of CO_2 and H_2O in d^3 and d^4 MXenes. The chemisorbed N_2 becomes activated, promoting its catalytic conversion into NH_3. The first proton–electron transfer is found to be the rate-determining step for the whole process, with an activation barrier of only 0.64 eV *vs.* SHE for V_3C_2.

Dinitrogen (N_2) constitutes about 78% of the atmosphere and plays a key role as a building block of amino and nucleic acids.[1] However, there is another undeniable landmark around the use of N_2, the Haber–Bosch process: the main industrial process for the production of ammonia (NH_3) from atmospheric N_2 and dihydrogen (H_2), at high temperatures and pressures.[2] The Haber–Bosch process has been acclaimed[3] as the most important discovery of the last century, given the impact of NH_3 in the fertilizer industry and as a precursor for nitrogen-containing compounds, among other applications.

Renewable N_2 conversion into NH_3 as a 'green fuel' technology is recently being considered as another possible alternative to fossil fuels. As stated by Nørskov and his co-workers,[4] the development of an efficient, realistic machinery for electrochemical N_2 conversion could provide an alternative route to NH_3 on a distributed basis, avoiding the key factors that require the Haber–Bosch process industry: intense conditions of temperature/pressure combined with a considerable, complex plant infrastructure.[5]

Broader context

Ammonia (NH_3) is increasingly being considered as a real substitute for petroleum as a transportation fuel. The energy stored in the N–H bonds from NH_3 can be exploited when combusted, leading to a highly exothermic process and producing harmless, zero-balance greenhouse products such as dinitrogen gas and water vapour. The heavy energy-consumption and the considerable, complex plant infrastructure that the classical Haber–Bosch process requires, make the electrochemical synthesis of NH_3 an alternative for a cheap and clean technology of paramount importance from both the industrial and environmental points-of-view. Our density functional theory (DFT) results hypothesise that 2D transition metal carbides, namely 'MXenes', are promising materials for N_2 capture, being even thermodynamically preferred over the capture of CO_2 and H_2O. Chemisorbed N_2 on MXenes experiences an elongation/weakness of the N≡N triple bond promoting its catalytic conversion into NH_3 under mild conditions. Specifically, N_2 activation can be spontaneously achieved when it is chemically adsorbed on MXene nanosheets, and overpotentials can be as low as 0.64 V and 0.90 V *vs.* SHE in the case of V_3C_2 and Nb_3C_2, respectively. Finally, our predictions may stimulate experimentalists to synthesize and test 2D carbides towards the development of energy-saving technology for NH_3 electrosynthesis.

Transition metal carbides,[6–10] also known as 'MXenes' due to their similarity to graphene, are a novel class of 2D materials synthesised *via* the exfoliation of strong primary bond-containing solids; for example, metal carbides or nitrides, such as Ti_3AlC_2 can be converted into Ti_3C_2 (an MXene) by sonication.[11] MXenes exhibit an inherent metallic character; however once the surface is –F or –OH terminated, they can act as semiconductors. Among a variety of properties, MXenes are notable for their similar conductivity to multilayer graphene, excellent stabilities, as well as hydrophilic properties.[6] Apart from the multitude of recent applications, including electrode applications in Li-ion[12,13] and Na-ion[14] batteries or electrochemical supercapacitors,[14–16] MXenes have also been tested as catalytic and electro-catalytic materials for water splitting, and hydro-processing technology.[17,18] The electro-catalytic applications arise from their promising properties including high specific areas,[19] good electrical conductivities, stability,[8,20–22] and hydrophilic behaviors.[6] In addition,

[a] *ARC Centre of Excellence for Electromaterials Science (ACES), School of Chemistry, Faculty of Science, Monash University, Clayton, VIC 3800, Australia. E-mail: Chenghua.Sun@monash.edu*

[b] *State Key Laboratory of Silicate Materials for Architectures, Wuhan University of Technology, Hubei, 430070, China*

† Electronic supplementary information (ESI) available: Full computational details, thermochemistry analysis, computation of activation barriers in electrochemical reactions, optimisation of lattice parameters in MXenes, Gibbs free energies, and optimised structures leading to an unambiguous reproducibility of the present outcomes. See DOI: 10.1039/c6ee01800a

2D MXene compounds have been recently demonstrated as CO oxidation catalysts.[23]

Recognising these properties, in this work we investigate the function of d^2 (M = Ti, Zr, and Hf), d^3 (M = V, Nb, and Ta), and d^4 (M = Cr and Mo) MXenes having the general formula M_3C_2 as N_2 capture materials that can promote its activation for electrochemical conversion into ammonia. The present work focuses on the unravelling of such a mechanism, and identifies the promising prospects for the V_3C_2 and Nb_3C_2 materials, in particular. Thus, some of these recently reported MXene materials[11] are profiled as alternatives to the cluster-based catalysts developed for N_2 conversion.[24–26] We begin with an investigation of the initial N_2 absorption and the activation step onto these surfaces and then proceed to analyse the mechanistic pathways that eventuate.

N_2 chemisorption

The first step of the N_2 conversion consists of the interaction of the N_2 molecule with the catalytic surface as a fundamental requisite to start the reactive process. Our DFT+D3 results‡ (full details provided in the ESI†) suggest that N_2 goes from the gas phase to a chemisorbed state in a spontaneous process without passing through a physisorbed minimum; that is, with negative changes of the Gibbs free energies (Table S3, ESI†). d^3 Ta_3C_2 and d^2 Ti_3C_2 exhibit large binding energies, −2.60 and −2.70 eV respectively, indicating a strong N_2-philicity of the materials. Similar results are also seen in the Nb_3C_2 and Zr_3C_2 cases, with values of −2.44 and −2.41 eV, respectively. The strength of the capture is somewhat lower for the rest of MXenes; however the values are still promising (−2.17, −2.12, −2.12, and −2.06 eV, for M = V, Hf, Mo, and Cr, in each M_3C_2 case. This trend in the N_2-philicity is observed to be in contrast to the potential applications of the catalysts in the electrochemical N_2 conversion into NH_3. As will be discussed in the next section, the stronger the capture of N_2, the higher is the limiting reaction energy (Table S3, ESI†) of the whole process in each MXene series.

Before making an in-depth analysis of the subsequent mechanisms, it is worth mentioning some other fundamental features concerning the N_2 chemisorption step. A comparison with the CO_2 and H_2O chemisorption events on these materials is informative. Fig. 1 shows the DFT+D3 calculated structures of bound N_2, CO_2, and H_2O on the surface of the MXenes. The d^2 MXenes exhibit an extraordinary CO_2-philicity, computed binding energies being −3.02, −3.10, −2.58 eV for M = Ti, Zr, and Hf, respectively. These values are larger than those calculated for the N_2 chemisorption, but lower than for H_2O capture (up to −0.80 eV). In the case of the d^3 and d^4 MXenes, the N_2 is preferred over CO_2 or H_2O chemisorption. For instance, on V_3C_2, N_2 is captured in a spontaneous process releasing 2.17 eV, whereas CO_2 and H_2O do so with 1.53 and 0.92 eV, respectively, suggesting a clear selectivity in favour of N_2 capture and offering encouraging perspectives for the use of these materials in an aqueous or humid environment. The predicted high

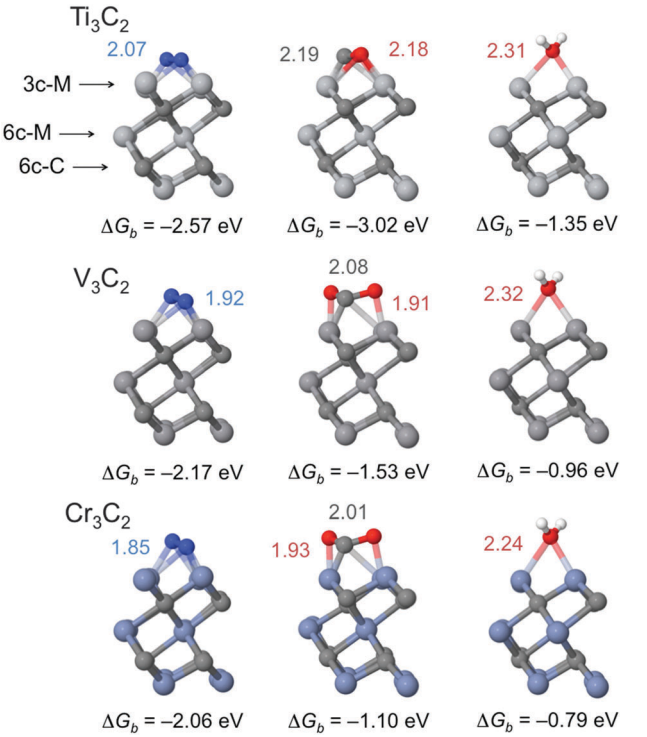

Fig. 1 N_2, CO_2, and H_2O chemisorbed minima captured by d^2 Ti_3C_2 (top), d^3 V_3C_2 (centre), and d^4 Cr_3C_2 (bottom) MXenes. Proximal $d_{N/C/O-M}$ distances (in Å) are indicated in blue, grey, and red colours, respectively. Gibbs free binding energies at T = 298.15 K, f = 101 325 Pa).

reactivity of transition metal carbides with the inert molecules like CO_2 has been demonstrated by recent modelling carried out by Illas and co-workers.[27]

From this, a major question arises: what is the origin of the strength of the N_2-philicity of M_3C_2 MXenes? Given that the N lone pairs (N_{lp}) from N_2 are weak interaction acceptors,[28] the nature of the strongly bounded state of N_2 on the MXenes must originate in other factors. As indicated from the optimized geometries in Fig. 1, the N–N bond length has been strongly elongated from 1.098 Å in the gas phase[29] to 1.35, 1.37, and 1.39 Å in the case of M = Ti, Zr, and Hf, indicating that a weakening of the triple N≡N bond by almost 0.30 Å. V_3C_2 and Nb_3C_2 exhibited smaller binding energies, with d_{NN} for the captured N_2 of 1.28 and 1.30 Å, respectively. It is worth noting that the N_2 dissociation step has been theoretically[30] and experimentally[31] proven to be the rate-limiting step of the Haber–Bosch process; in the present case, the weakening of the triple N≡N bond, and therefore its activation, is spontaneous.

N_2 reduction mechanism

Recent investigations carried out by Anderson *et al.*[32] have proposed the existence of two different mechanisms for the electrochemical N_2 conversion into NH_3 when catalysed by the tris(phosphine)borane-supported iron complex. On the one hand (path 2, Scheme S1, ESI†), three successive H^+/e^- pair gains are postulated to successively occur on one of the two N centres

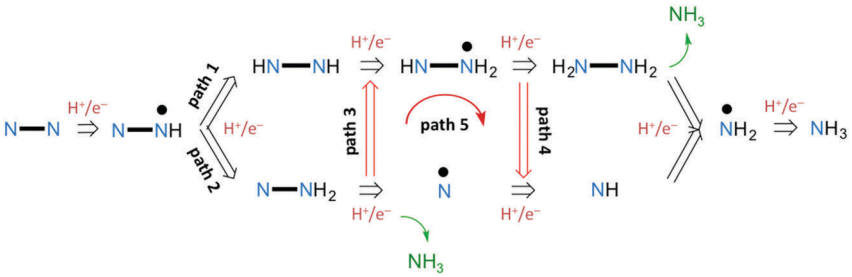

Scheme 1 Proposed routes for the N_2 conversion mechanism.

from N_2, producing the release of one NH_3 molecule and forming a single N atom that is finally converted into a second NH_3 molecule. On the other hand, the diazene–hydrazine–ammonia pathway (path 1, Scheme 1) is conjectured to be an alternative mechanism.

To investigate the mechanisms of N_2 reduction on these MXene materials we have carried out DFT+D3 calculations on periodic $M_{12}C_8$ super-cells‡ (full details provided in the ESI†). The data are collected at the Gibbs free energy section from the ESI† and some selected examples of the results are presented in Fig. 2. We identified and explored five possible mechanisms, as summarised in Scheme 1. These include those postulated by Anderson *et al.*,[32] and the single-double cross-over routes before and/or after the third hydrogenation step towards the formation of the plausible HN–NH_2• or N• radicals. In general, although all products and intermediate species have been theoretically found to be stable entities, two different mechanistic behaviours can be discriminated in the studied materials. On the one hand, the d^2 M_3C_2 materials are found to prefer the pathway through HN–NH and HN–NH_2• (the second- and third-hydrogenated species), *i.e.* path 4, whereas for the d^3 and d^4 M_3C_2 surfaces, the N–NH_2 and N• species (path 2) are preferred along their minimum energy paths (see Table S3 in the ESI†).

Comparison of the reaction energies and transition states in the pathways demonstrates that V_3C_2 and Nb_3C_2 materials are the most promising candidates for the electrochemical N_2 conversion. The largest reaction energies for V_3C_2 and Nb_3C_2 materials are only 0.32 and 0.39 eV *vs.* the Standard Hydrogen Electrode

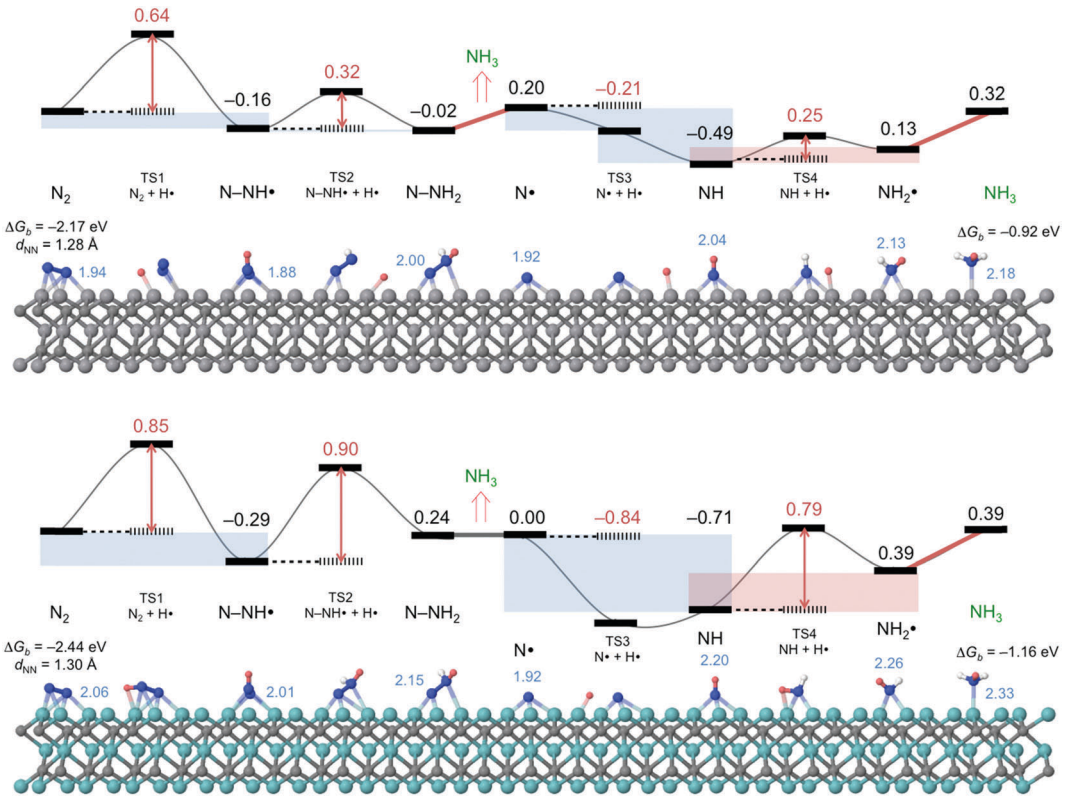

Fig. 2 Minimum energy path for the N_2 conversion into NH_3 catalysed by V_3C_2 (top) and Nb_3C_2 (bottom) MXenes, calculated at the DFT+D3 computational level. Structures and energies of the intermediates and transition states (TS) indicated. Gibbs free reaction (black text) and activation (red text) energies, *vs.* SHE [pH = 0, $f(H_2)$ = 101 325 Pa, and U = 0 V], at T = 298.15 K, are shown in eV. Selected d_{MN} distances are shown in Å. Reactive hydrogen atom during the N_2 electro-reduction is highlighted in pink in each step. Shading indicates spontaneous (blue) *versus* non-spontaneous (red) steps.

(SHE, hereby extensive to all electro-chemical H^+/e^- additions), respectively, and as shown in Fig. 2, they arise from the sixth H^+/e^- pair gain in order to produce NH_3 from the $NH_2^\bullet$ intermediate species. Cr_3C_2 and to some extent Mo_3C_2 also offer potentially good catalytic performance. This is not the case for the d^2 series of MXenes, as well as Ta_3C_2, since reaction energy impediments around 1.5 eV and 0.99 eV, respectively, appear in these cases.

Generally, the first hydrogenation of N_2 to form the $N–NH^\bullet$ radical demands a substantial energy input in an isolated transformation. For instance, the electron affinity for an isolated N_2 molecule generating $N_2^{\bullet-}$ has been estimated as 1.98 eV at the CCSD(T) = full/aug-cc-pVQZ level of theory.[33] On the other hand, in the MXene materials, we instead observe spontaneous reaction energies, of −0.16 and −0.29 eV when M = V and Nb.

However, at this point it is also vital to analyse the effect of kinetic factors *via* an investigation of the transition states in a process such as this. Our DFT+D3 calculations have also identified the transition states (TS's) and their structures and energies. The results, also shown in Fig. 2 and detailed in Table S5 (ESI†), indicate activation barriers of 0.64 (V_3C_2) and 0.85 eV (Nb_3C_2) for the first transition state (TS1, $N_2 + H^\bullet$) that connects N_2 and $N–NH^\bullet$. Considering the minimum energy path shown in Fig. 2, it seems that this kinetic impediment is the rate-determining step of the whole process for V_3C_2 and the one corresponding with the second hydrogenation step (0.90 eV) for Nb_3C_2. In other words, it appears that once N_2 is spontaneously captured by V_3C_2 and Nb_3C_2, limiting barriers of just 0.64 and 0.90 V are demanded for its electrochemical conversion into NH_3.

It should be highlighted that, in addition to its better catalytic performance, V_3C_2 also exhibits a smoother reaction profile along the rest of the N_2 electro-chemical conversion mechanism. For instance, TS2 and TS4, the transition states leading to the $N–NH_2$ and $NH_2^\bullet$ intermediate species respectively, exhibit activation barriers of only 0.32 and 0.25 eV, while for Nb_3C_2, these increase to 0.90 and 0.79 eV, respectively. Also interesting is the case of TS3 in which the electrochemical reduction of $N^\bullet$ to reach NH is found to be a barrier-less process, a behaviour which is observed for both V_3C_2 and Nb_3C_2 MXenes.

Finally, the release of the chemisorbed NH_3 as a result of the sixth H^+/e^- pair gain demands the injection of 0.92 and 1.16 eV, respectively. However, in a flowing N_2 environment the NH_3 product would be steadily removed by constant equilibration with the gas phase.

In summary, our state-of-the-art DFT+D3 calculations on M_3C_2 transition metal carbides from the d^2 (M = Ti, Zr, and Hf), d^3 (M = V, Nb, and Ta), and d^4 (M = Cr and Mo) series have demonstrated that these materials are promising for N_2 capture and reduction. The large spontaneous Gibbs free binding energies have been obtained for N_2 chemisorption, being even larger than those corresponding to the capture of CO_2 in the d^3 and d^4 MXenes, and for H_2O in all cases. N_2 becomes activated *via* its capture, and the V_3C_2 and Nb_3C_2 materials exhibit the most promising features for reduction to NH_3, with maximum over-potentials of 0.64 and 0.90 V *vs.* SHE, respectively. These limiting kinetic barriers are imposed by the transition state involved in the first and second H^+/e^- pair gains to form the $N–NH^\bullet$ and $N–NH_2$ species in V_3C_2 and Nb_3C_2, respectively.

The authors acknowledge the Australian Research Council (ARC) for CS's Future Fellowship and DRM's Laureate Fellowship, and the National Natural Science Foundation of China for supporting our research. We also thank the National Computational Infrastructure (NCI), and the National Energy Research Scientific Computing Center in Shanghai, for providing the computational resources. Special gratitude is due to Prof. Dr Michael J. Janik (PennState) for his advice in the estimation of activation barriers in electrochemical reactions.[34]

Notes and references

‡ Method: density functional theory (DFT) through the generalized gradient approximation (GGA) using the Perdew–Burke–Ernzerhof (PBE) functional. Inclusion of explicit dispersion corrections implemented through the use of the D3 method with the standard parameters programmed by Grimme and co-workers. Searching of transition states (TS) carried out *via* the nudge elastic band (NEB) method. See full details in the Computational details section of the ESI.†

1 A. Bernhard, *Nat. Educ. Knowl.*, 2010, **3**, 25.
2 M. Appl, *Ammonia – Ullmann's Encyclopedia of Industrial Chemistry*, Wiley-VCH Verlag GmbH & Co. KGaA, 2002.
3 V. Smil, *Nature*, 1999, **400**, 415.
4 J. H. Montoya, C. Tsai, A. Vojvodic and J. K. Nørskov, *ChemSusChem*, 2015, **8**, 2180.
5 R. Schlögl, *Angew. Chem., Int. Ed.*, 2003, **42**, 2004.
6 M. Naguib, O. Mashtalir, J. Carle, V. Presser, J. Lu, L. Hultman, Y. Gogotsi and M. W. Barsoum, *ACS Nano*, 2012, **6**, 1322.
7 M. Naguib, J. Halim, J. Lu, K. M. Cook, L. Hultman, Y. Gogotsi and M. W. Barsoum, *J. Am. Chem. Soc.*, 2013, **135**, 15966.
8 M. Naguib, V. N. Mochalin, M. W. Barsoum and Y. Gogotsi, *Adv. Mater.*, 2014, **26**, 992.
9 J. Yang, M. Naguib, M. Ghidiu, L.-M. Pan, J. Gu, J. Nanda, J. Halim, Y. Gogotsi and M. W. Barsoum, *J. Am. Ceram. Soc.*, 2016, **99**, 660.
10 B. Anasori, Y. Xie, M. Beidaghi, J. Lu, B. C. Hosler, L. Hultman, P. R. C. Kent, Y. Gogotsi and M. W. Barsoum, *ACS Nano*, 2015, **9**, 9507.
11 M. Naguib, M. Kurtoglu, V. Presser, J. Lu, J. Niu, M. Heon, L. Hultman, Y. Gogotsi and M. W. Barsoum, *Adv. Mater.*, 2011, **23**, 4248.
12 Y. Xie, M. Naguib, V. N. Mochalin, M. W. Barsoum, Y. Gogotsi, X. Yu, K.-W. Nam, X.-Q. Yang, A. I. Kolesnikov and P. R. C. Kent, *J. Am. Chem. Soc.*, 2014, **136**, 6385.
13 X. Liang, A. Garsuch and L. F. Nazar, *Angew. Chem., Int. Ed.*, 2015, **54**, 3907.
14 D. Er, J. Li, M. Naguib, Y. Gogotsi and V. B. Shenoy, *ACS Appl. Mater. Interfaces*, 2014, **6**, 11173.
15 M. R. Lukatskaya, O. Mashtalir, C. E. Ren, Y. Dall'Agnese, P. Rozier, P. L. Taberna, M. Naguib, P. Simon, M. W. Barsoum and Y. Gogotsi, *Science*, 2013, **341**, 1502.

16 M. Ghidiu, M. R. Lukatskaya, M.-Q. Zhao, Y. Gogotsi and M. W. Barsoum, *Nature*, 2014, **516**, 78.
17 E. Furimsky, *Appl. Catal., A*, 2003, **240**, 1.
18 W. F. Chen, C. H. Wang, K. Sasaki, N. Marinkovic, W. Xu, J. T. Muckerman, T. Zhu and R. R. Adzic, *Energy Environ. Sci.*, 2013, **6**, 943.
19 J. S. Lee, *Metal Carbides – Encyclopedia of Catalysis*, John Wiley & Sons, Inc., 2002.
20 X. Xie, S. Chen, W. Ding, Y. Nie and Z. Wei, *Chem. Commun.*, 2013, **49**, 10112.
21 A. N. Enyashin and A. L. Ivanovskii, *J. Phys. Chem. C*, 2013, **117**, 13637.
22 O. Mashtalir, K. M. Cook, V. N. Mochalin, M. Crowe, M. W. Barsoum and Y. Gogotsi, *J. Mater. Chem. A*, 2014, **2**, 14334.
23 X. Zhang, J. Lei, D. Wu, X. Zhao, Y. Jing and Z. Zhou, *J. Mater. Chem. A*, 2016, **4**, 4871.
24 J. S. Anderson, M.-E. Moret and J. C. Peters, *J. Am. Chem. Soc.*, 2013, **135**, 534.
25 S. E. Creutz and J. C. Peters, *J. Am. Chem. Soc.*, 2014, **136**, 1105.
26 A. Banerjee, B. D. Yuhas, E. A. Margulies, Y. Zhang, Y. Shim, M. R. Wasielewski and M. G. Kanatzidis, *J. Am. Chem. Soc.*, 2015, **137**, 2030.
27 C. Kunkel, F. Viñes and F. Illas, *Energy Environ. Sci.*, 2016, **9**, 141.
28 S. Begum and R. Subramanian, *Phys. Chem. Chem. Phys.*, 2014, **16**, 17658.
29 K. P. Huber and G. Herzberg, *Molecular Spectra and Molecular Structure. IV. Constants of Diatomic Molecules*, Van Nostrand Reinhold Co., 1979.
30 K. Honkala, A. Hellman, I. N. Remediakis, A. Logadottir, A. Carlsson, S. Dahl, C. H. Christensen and J. K. Nørskov, *Science*, 2005, **307**, 555.
31 S. Dahl, P. A. Taylor, E. Törnqvist and I. Chorkendorff, *J. Catal.*, 1998, **178**, 679.
32 J. S. Anderson, J. Rittle and J. C. Peters, *Nature*, 2013, **501**, 84.
33 See NIST database at: http://cccbdb.nist.gov/.
34 X. Nie, M. R. Esopi, M. J. Janik and A. Asthagiri, *Angew. Chem., Int. Ed.*, 2013, **52**, 2459.